Available online at www.sciencedirect.com

ScienceDirect

Procedia Structural Integrity 2 (2016) 3447–3458

Structural Integrity Procedia

www.elsevier.com/locate/procedia

21st European Conference on Fracture, ECF21, 20-24 June 2016, Catania, Italy

Crack propagation in layers under small-scale yielding

J. P. Vafa, S. J. Fariborz*

Department of Mechanical Engineering, Amirkabir University of Technology (Tehran Polytechnic), 424, Hafez Avenue, Tehran 158754413, Iran

Abstract

The stress field is obtained in an isotropic elastic layer containing an edge dislocation. The dislocation solution is used to derive integral equations for a cracked layer. These are a set of Cauchy singular integral equations which are solved numerically for the density of dislocations on a crack surface. The density of dislocations is utilized to determine stress components in the vicinity of a crack tip. The stress field contains singular as well as non-singular terms. Assuming small scale yielding, the von-Mises yield criterion is adopted to define a plastic region around a crack tip under the plane-stress situation. Several examples are solved and the plastic region developed by a crack with different orientations and loadings is specified. Moreover, in another example, plastic regions around the tips of two interacting cracks are defined. The geometry of the plastic regions is utilized to obtain a crack propagation angle.

Keywords: Elastic layer; Multiple cracks; Plastic region; Crack propagation angle.

1. Introduction

The extent of a plastic region around a crack tip is of utmost importance in the fracture behavior of metallic structures [Banks and Garlick (1984)]. It is well-known that in ductile materials plastic zone around a crack tip has a shielding effect; hence, enhances the material resistance against crack driving force [Zhu et al (2010)]. The shape and size of a plastic zone around a crack tip was used by, Golos and Wasiluk (2000), and Bian and Kim (2004), to evaluate the angle of crack propagation under mixed mode deformation.

* Corresponding author. Tel.: +98 2164543460; fax: +98 2166419736.
E-mail address: sjfariborz@yahoo.com

10.1016/j.prostr.2016.06.430

Nomenclature

b_{ni}	density functions of the climb dislocation on the i_{th} crack
b_{si}	density functions of the glide dislocation on the i_{th} crack
B_x	x component of Burgers vector
B_y	y component of Burgers vector
h	layer thickness
H	Heaviside function
L	Crack length
N	number of cracks
n	unit vector normal to crack surface
R	radius around crack tip
s	unit vector tangential to crack surface
u	displacement component
v	displacement component
η	y coordinate of dislocation point
η_i	y component of i_{th} curve parametric equation
θ	crack propagation angle
θ_i	angle between crack and x axes
κ	Kolosov constant
μ	shear modulus of elasticity
ν	Poisson's ratio
ξ	x coordinate of dislocation point
ξ_i	x component of i_{th} curve parametric equation
σ_{ij}	stress field components
$\bar{\sigma}_{ij}$	stress components due to external traction
σ_Y	yield stress of material
σ_θ	tangential stress

Khan and Khraisheh (2000) based upon the extent of plastic region introduced a plastic region with variable radius which was incorporated in the formulation of the maximum tangential stress criterion to make it applicable for ductile materials. Moreover, a plastic zone significantly influences crack growth under fatigue conditions [Harmain and Provan (1997)]. Dugdale (1960), considered the plastic zone as a thin strip forming ahead of a crack tip based on experimental observation of stationary cracks in thin steel sheets under mode I condition. Dugdale's model has been modified and used by several investigators to include mixed mode deformation, Panasyuk and Savruk (1992), and Neimitz (2004). Larsson and Carlsson (1973) used the finite element method for mode I elastic-plastic analysis of cracks. They claimed that in addition to the singular term of elastic stress solution the non-singular term is required for the definition of plastic region.

In all the above studies dealing with mixed mode fracture, only the singular terms of stress components were used to define the plastic region around a crack tip. Moreover, infinite planes with a single crack were studied and the analysis may not be extended to multiple cracks. In the present work, based on the definition of Volterra edge dislocation the integral equations are derived for the density of dislocations on the surfaces of multiple cracks in an elastic layer. This allows the determination of stress fields around a crack tip under mixed mode conditions. Under the hypothesis of small scale yielding and in conjunction with von-Mises yield criterion plastic region is specified around a crack tip. The effects of geometry of cracks, loading and interaction between cracks on the plastic region are investigated. Furthermore, using the geometry of plastic region the angle at which a crack may propagate is evaluated.

2. Dislocation solution

In the plane infinitesimal theory of elasticity, the constitutive equations for isotropic materials are expressed as

$$\sigma_{xx} = \frac{\mu}{\kappa-1}\left[(\kappa+1)\frac{\partial u}{\partial x} + (3-\kappa)\frac{\partial v}{\partial y}\right]$$

$$\sigma_{yy} = \frac{\mu}{\kappa-1}\left[(\kappa+1)\frac{\partial v}{\partial y} + (3-\kappa)\frac{\partial u}{\partial x}\right]$$

$$\sigma_{xy} = \mu\left(\frac{\partial u}{\partial y} + \frac{\partial v}{\partial x}\right) \tag{1}$$

The Kolosov constant is $\kappa = 3-4\nu$ for plane strain and $\kappa = (3-\nu)/(1+\nu)$ for plane stress situations. Substitution of Eqs (1) into the equilibrium equations $\sigma_{ij,j} = 0,\ i,j \in \{x,y\}$ results in the Navier's equations as

$$\frac{\partial^2 u}{\partial x^2} + \frac{\partial^2 u}{\partial y^2} + \frac{2}{\kappa-1}\frac{\partial}{\partial x}\left(\frac{\partial u}{\partial x} + \frac{\partial v}{\partial y}\right) = 0$$

$$\frac{\partial^2 v}{\partial x^2} + \frac{\partial^2 v}{\partial y^2} + \frac{2}{\kappa-1}\frac{\partial}{\partial y}\left(\frac{\partial u}{\partial x} + \frac{\partial v}{\partial y}\right) = 0 \tag{2}$$

We consider a layer with thickness h containing a Volterra edge dislocation situated at (ξ,η). The Burgers vector of dislocation is identified by its components B_x and B_y representing glide and climb of the dislocation, respectively. The dislocation cut is a semi-infinite line which is extended on the positive x-direction. The dislocation may be identified as

$$u(x,\eta^+) - u(x,\eta^-) = B_x H(x-\xi)$$

$$v(x,\eta^+) - v(x,\eta^-) = B_y H(x-\xi) \tag{3}$$

The continuity of traction on the dislocation cut requires that

$$\sigma_{yy}(x,\eta^+) = \sigma_{yy}(x,\eta^-)$$

$$\sigma_{xy}(x,\eta^+) = \sigma_{xy}(x,\eta^-) \tag{4}$$

Moreover, the traction free condition on the layer surface implies

$$\sigma_{yy}(x,0) = \sigma_{yy}(x,h) = 0$$

$$\sigma_{xy}(x,0) = \sigma_{xy}(x,h) = 0 \tag{5}$$

Application of the complex Fourier transform to Eqs. (2), subjected to conditions (3)-(5), results in the stress components

$$\sigma_{ij}(x,y,\xi,\eta) = B_x k_{ij}^x(x,y,\xi,\eta) + B_y k_{ij}^y(x,y,\xi,\eta),\ i,j \in \{x,y\} \tag{6}$$

where k_{ij}^x, k_{ij}^y are given in the Appendix A. Let the layer be weakened by N curved cracks which are expressed in parametric form

$$\begin{cases} x_i = \xi_i(p) \\ y_i = \eta_i(p) \end{cases} \qquad -1 \le p \le 1, \quad i \in \{1,2,\dots,N\} \tag{7}$$

Cracks subjected to in-plane loads may be modeled by the distribution of edge dislocations on their surfaces. Let b_{ni} and b_{si} represent, respectively, the density functions of the climb and glide of dislocations on the i_{th} crack. The components of Burgers vector may be transformed as

$$\begin{Bmatrix} b_{xi} \\ b_{yi} \end{Bmatrix} dx = \begin{bmatrix} cos(\theta_i) & -sin(\theta_i) \\ sin(\theta_i) & cos(\theta_i) \end{bmatrix} \begin{Bmatrix} b_{si} \\ b_{ni} \end{Bmatrix} ds \tag{8}$$

From Eqs (6) and (8) the components of traction vector on the surface of i_{th} crack due to distribution of dislocations on all N cracks become

$$\bar{\sigma}_{ni}\big(x_i(p), y_i(p)\big) = \sum_{j=1}^{N} \int_{-1}^{1} \Big[K_{11}\Big(x_i(p), y_i(p), \xi_j(q), \eta_j(q)\Big) b_{nj}(q) + K_{12}\Big(x_i(p), y_i(p), \xi_j(q), \eta_j(q)\Big) b_{sj}(q)\Big] \sqrt{\big[\xi_j'(q)\big]^2 + \big[\eta_j'(q)\big]^2}\, dq$$

$$\bar{\sigma}_{si}\big(x_i(p), y_i(p)\big) = \sum_{j=1}^{N} \int_{-1}^{1} \Big[K_{21}\Big(x_i(p), y_i(p), \xi_j(q), \eta_j(q)\Big) b_{nj}(q) + K_{22}\Big(x_i(p), y_i(p), \xi_j(q), \eta_j(q)\Big) b_{sj}(q)\Big] \sqrt{\big[\xi_j'(q)\big]^2 + \big[\eta_j'(q)\big]^2}\, dq\,, \ i \in \{1,2,\dots,N\} \tag{9}$$

In Eq. (9) and henceforth, prime indicates derivative with respect to the argument. Using Eqs (6) and (8), we arrive at the kernels of integral Eqs (9)

$$K_{11}(x,y,\xi,\eta) = -sin^2[\theta_i(p)]\, sin\big[\theta_j(q)\big]\, k_{xx}^{x}(x,y,\xi,\eta) + sin^2[\theta_i(p)]\, cos\big[\theta_j(q)\big]\, k_{xx}^{y}(x,y,\xi,\eta) - cos^2[\theta_i(p)]\, sin\big[\theta_j(q)\big]\, k_{yy}^{x}(x,y,\xi,\eta) + cos^2[\theta_i(p)]\, cos\big[\theta_j(q)\big]\, k_{yy}^{y}(x,y,\xi,\eta) + sin[2\theta_i(p)]\, sin\big[\theta_j(q)\big]\, k_{xy}^{x}(x,y,\xi,\eta) - sin[2\theta_i(p)]\, cos\big[\theta_j(q)\big]\, k_{xy}^{y}(x,y,\xi,\eta)$$

$$K_{12}(x,y,\xi,\eta) = sin^2[\theta_i(p)]\, cos\big[\theta_j(q)\big]\, k_{xx}^{x}(x,y,\xi,\eta) + sin^2[\theta_i(p)]\, sin\big[\theta_j(q)\big]\, k_{xx}^{y}(x,y,\xi,\eta) + cos^2[\theta_i(p)]\, cos\big[\theta_j(q)\big]\, k_{yy}^{x}(x,y,\xi,\eta) + cos^2[\theta_i(p)]\, sin\big[\theta_j(q)\big]\, k_{yy}^{y}(x,y,\xi,\eta) - sin[2\theta_i(p)]\, cos\big[\theta_j(q)\big]\, k_{xy}^{x}(x,y,\xi,\eta) - sin[2\theta_i(p)]\, sin\big[\theta_j(q)\big]\, k_{xy}^{y}(x,y,\xi,\eta)$$

$$K_{21}(x,y,\xi,\eta) = \frac{1}{2} sin[2\theta_i(p)]\, sin\big[\theta_j(q)\big]\, k_{xx}^{x}(x,y,\xi,\eta) - \frac{1}{2} sin[2\theta_i(p)]\, cos\big[\theta_j(q)\big]\, k_{xx}^{y}(x,y,\xi,\eta) - \frac{1}{2} sin[2\theta_i(p)]\, sin\big[\theta_j(q)\big]\, k_{yy}^{x}(x,y,\xi,\eta) + \frac{1}{2} sin[2\theta_i(p)]\, cos\big[\theta_j(q)\big]\, k_{yy}^{y}(x,y,\xi,\eta) - cos[2\theta_i(p)]\, sin\big[\theta_j(q)\big]\, k_{xy}^{x}(x,y,\xi,\eta) + cos[2\theta_i(p)]\, cos\big[\theta_j(q)\big]\, k_{xy}^{y}(x,y,\xi,\eta)$$

$$K_{22}(x,y,\xi,\eta) = -\frac{1}{2} sin[2\theta_i(p)]\, cos\big[\theta_j(q)\big]\, k_{xx}^{x}(x,y,\xi,\eta) - \frac{1}{2} sin[2\theta_i(p)]\, sin\big[\theta_j(q)\big]\, k_{xx}^{y}(x,y,\xi,\eta) + \frac{1}{2} sin[2\theta_i(p)]\, cos\big[\theta_j(q)\big]\, k_{yy}^{x}(x,y,\xi,\eta) + \frac{1}{2} sin[2\theta_i(p)]\, sin\big[\theta_j(q)\big]\, k_{yy}^{y}(x,y,\xi,\eta) + cos[2\theta_i(p)]\, cos\big[\theta_j(q)\big]\, k_{xy}^{x}(x,y,\xi,\eta) + cos[2\theta_i(p)]\, sin\big[\theta_j(q)\big]\, k_{xy}^{y}(x,y,\xi,\eta) \tag{10}$$

In addition, for embedded cracks dislocation densities should satisfy the following closure requirement

$$\int_{-1}^{1} [cos[\theta_i(-1) - \theta_i(q)]\, b_{si}(q) - sin[\theta_i(-1) - \theta_i(q)]\, b_{ni}(q)] \sqrt{[\xi_i'(q)]^2 + [\eta_i'(q)]^2}\, dq = 0$$

$$\int_{-1}^{1} [sin[\theta_i(-1) - \theta_i(q)]\, b_{si}(q) + cos[\theta_i(-1) - \theta_i(q)]\, b_{si}(q)] \sqrt{[\xi_i'(q)]^2 + [\eta_i'(q)]^2}\, dq = 0, \ i \in \{1,2,\dots,N\} \tag{11}$$

The left-hand sides of Eqs (9), with opposite sign, are the stress components caused by applied traction on the presumed cracks surfaces in the intact layer. The system of integral equations (9) and (11) are solved by means of the

numerical procedure devised by Erdogan et al. (1973) to obtain the density of dislocations on a crack surface. The stress components at a point in the cracked layer are

$$\sigma_{ij}(x,y) = \sum_{m=1}^{N} \int_{-1}^{1} \Big(k_{ij}^{x}[x,y,\xi_m(q),\eta_m(q)]\{b_{sm}(q)\cos[\theta_m(q)] - b_{nm}(q)\sin[\theta_m(q)]\} + k_{ij}^{y}[x,y,\xi_m(q),\eta_m(q)]\{b_{sm}(q)\sin[\theta_m(q)] + b_{nm}(q)\cos[\theta_m(q)]\} \Big) \sqrt{[\xi_m'(q)]^2 + [\eta_m'(q)]^2}\, dq + \bar{\sigma}_{ij}(x,y), i,j \in \{x,y\} \quad (12)$$

3. Plastic region and crack propagation angle

The von-Mises yield criterion for incipient plastic flow under plane-stress condition is

$$\sigma_{xx}^2 + \sigma_{yy}^2 - \sigma_{xx}\sigma_{yy} + 3\tau_{xy}^2 = \sigma_Y^2 \quad (13)$$

The value of Poisson's ratio of the material is taken as $\nu = 0.3$. The stress field obtained from Eq. (12) should be substituted into (13) to define the boundary of the plastic region. It is worth mentioning that as we approach the crack flanks convergence of the results becomes problematic; thus the yielding point on a crack surface may not be specified accurately. For measuring the dimensions of the plastic regions circles are drawn with radius R, defined on the figures, centering at a crack tip and engulfing the plastic region. In the first example, the layer is weakened by a central crack with length $L = h/5$. The layer is subjected to constant normal traction $\sigma_{yy} = \sigma_Y/10$. Due to the symmetry of the problem with respect to crack only mode I fracture exists. The plastic region together with that of a crack in an infinite plane under identical load is depicted in Fig.1.

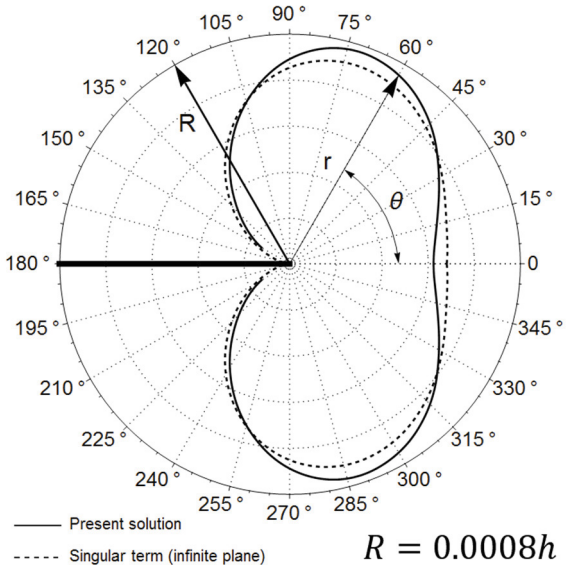

Fig. 1 Plastic zone for a small central crack

Since the crack is small in comparison with the layer thickness the plastic regions in the two cases are close and the difference may be attributed to the effects of non-singular terms of the stress field, in the cracked layer. In this example, it is well-known that a crack propagates along its line. However, we observe that tangential stress σ_θ, on the boundary of plastic region, is positive only for $0 \le \theta < 2\pi/3$ and $4\pi/3 < \theta \le 2\pi$ and at $\theta = 0$ the distance r is minimal. Therefore, we conceive that a crack propagates along the shorts line joining the crack tip to the boundary of

the plastic region wherein tangential stress is tensile, i.e. $\sigma_\theta > 0$. In the case of existence of more than one point on the boundary of a plastic region then, crack branching will occur.

In all the proceeding examples, layers are weakened by large cracks with length, $L = h/2$. The second example deals with a layer containing a crack parallel to the layer boundary. Three different locations for the crack are considered, Fig. 2.

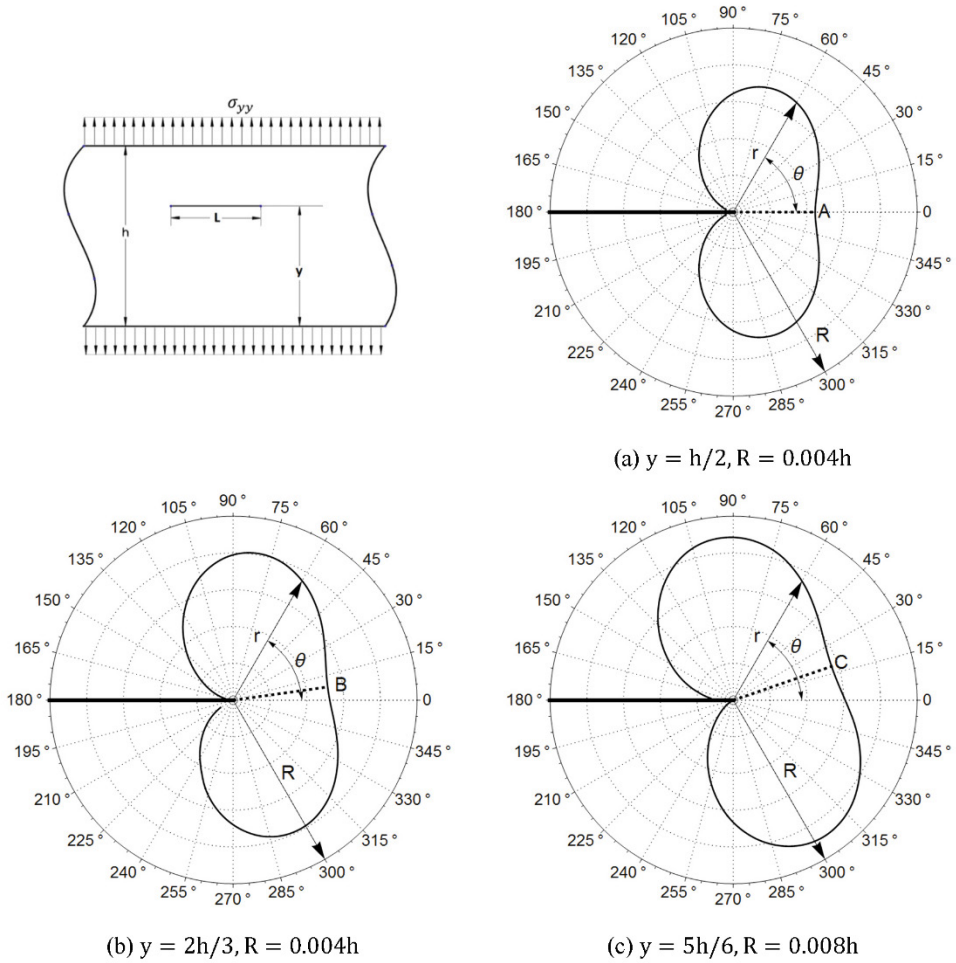

Fig. 2 Plastic zone and propagation angle for a crack parallel to the layer boundary

The loading is identical with the previous example. The off-center cracks experience mixed mode fracture. The plastic region is larger for a crack closer to the layer boundary. Using the aforementioned procedure, crack propagation angles are obtained as $\theta_A = 0, \theta_B = 8°$ and $\theta_C = 19°$. In order to compare our results with other crack propagation criteria another analysis is carried out. We observed that, on the surrounding circle, the nonsingular terms of stress components are much smaller than that of the singular ones. This allows the application of the maximum tangential stress criterion which only utilizes the singular terms of stress field. The criterion was devised by Erdogan and Sih (1963) for the predication of a crack propagation angle in brittle materials under mixed mode conditions. To this end, plots of tangential stress on the circles surrounding the plastic regions are provided, Fig. 3. As we may observe, the results of the two procedures are very close.

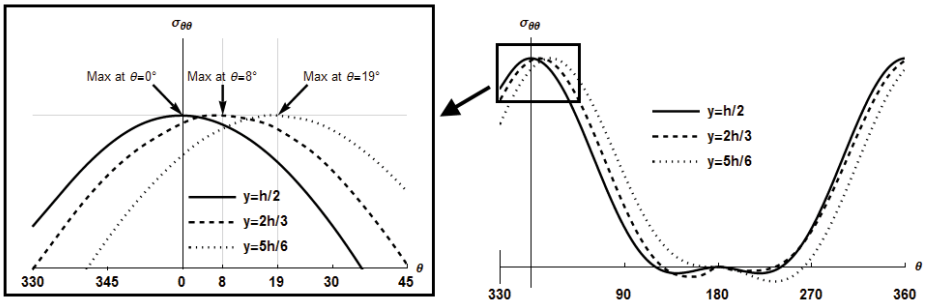

Fig. 3 Plots of tangential stress on the surrounding circles with radius R

In Fig. 4, layer is weakened by a crack situated at two different locations, $y = h/2$ and $y = 5h/6$. Constant shear traction $\tau_{xy} = \sigma_Y/10$ is applied on the layer boundary. Only mode II fracture occurs in the central crack whereas off-center crack is under mixed mode deformation. A portion of crack surface experiences plastic deformation. In Fig. 4a, the plastic region in a cracked infinite plane subjected to shear stress is drawn, as well. In the region around $\theta = \pi/2$ the tangential stress is compressive. Therefore, the angles of propagation of cracks are $\theta_A = 277°$ and $\theta_B = 284°$. We should mention that the value of θ_A is in the range of the values obtained by different criteria [Khan and Khraisheh (2000)] for the propagation of a crack under shear in ductile materials.

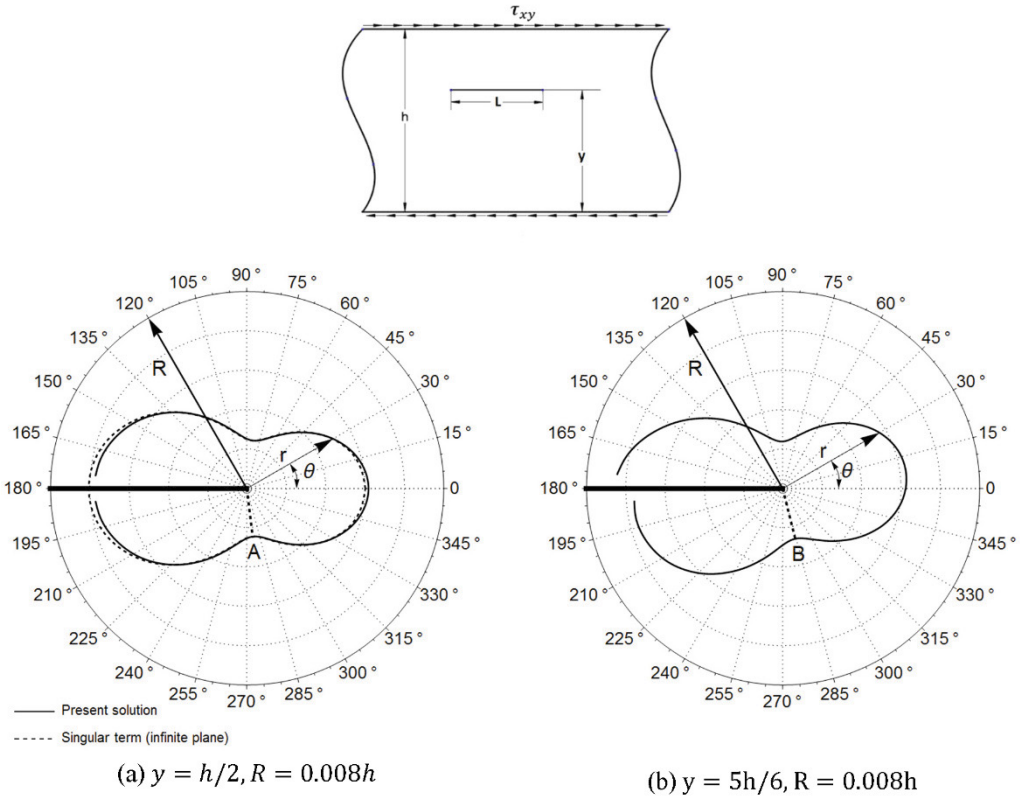

(a) $y = h/2, R = 0.008h$ (b) $y = 5h/6, R = 0.008h$

Fig. 4 Plastic zone and propagation angle for a crack parallel to the layer boundary

We analyze a cracked layer under normal and shear tractions $\sigma_{yy} = 2\tau_{xy} = \sigma_Y/10$. Three different orientations for the crack are considered while its center is fixed on the center-line of the layer Fig. 5. In all cases, mixed mode fracture prevails. Plot of plastic region of the crack situated in an infinite plane, wherein only singular terms exit, is compared with that of the central crack and shows no resemblance. Consequently, in a layer, for large cracks, non-singular terms of stress components should not be overlooked. As the crack angle increases stress field around a crack tip reduces leading to a smaller plastic region. In an oblique crack, however, plastic region covers a portion of crack surface. In the region between $\theta = 75°$ and the crack surface, tangential stress, $\sigma_\theta < 0$; thus, angles at which cracks propagate are $\theta_A = 327°, \theta_B = 326°$, and $\theta_C = 323°$.

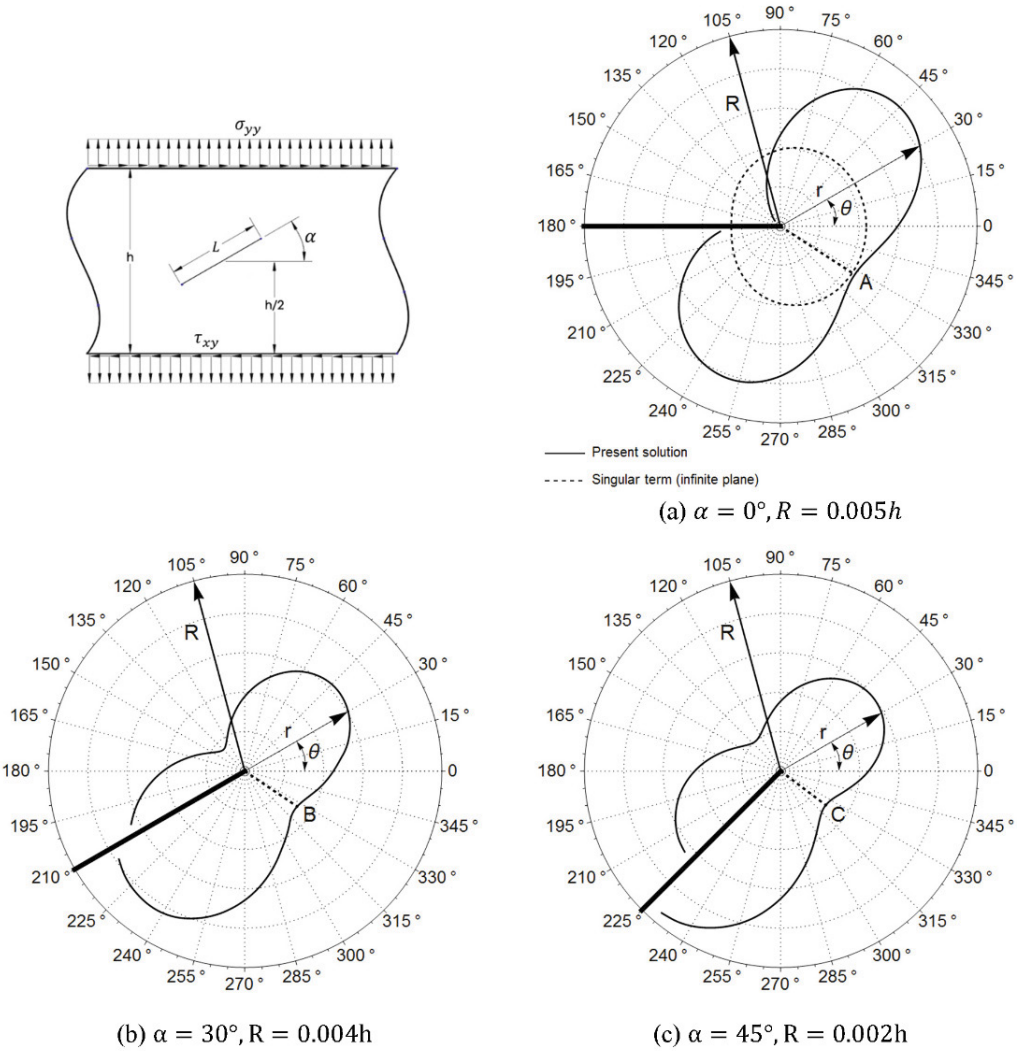

Fig. 5 Plastic zone and propagation angle for an oblique crack

In the last example, the interaction between a central and an oblique crack is studied, Fig. 6. The load on the layer is that of the previous example. Comparison of Figs 5a and 6a reveals the growth of the plastic region in this case. This is attributed to the strong interaction between cracks. In Figs 6a and 6b, respectively, for $75° < \theta < 180°$ and $\theta > 225°$ tangential stress is negative and cracks propagation angles are, $\theta_A = 327°$ and $\theta_B = 147°$. Thus, cracks propagate in opposite directions on two parallel lines.

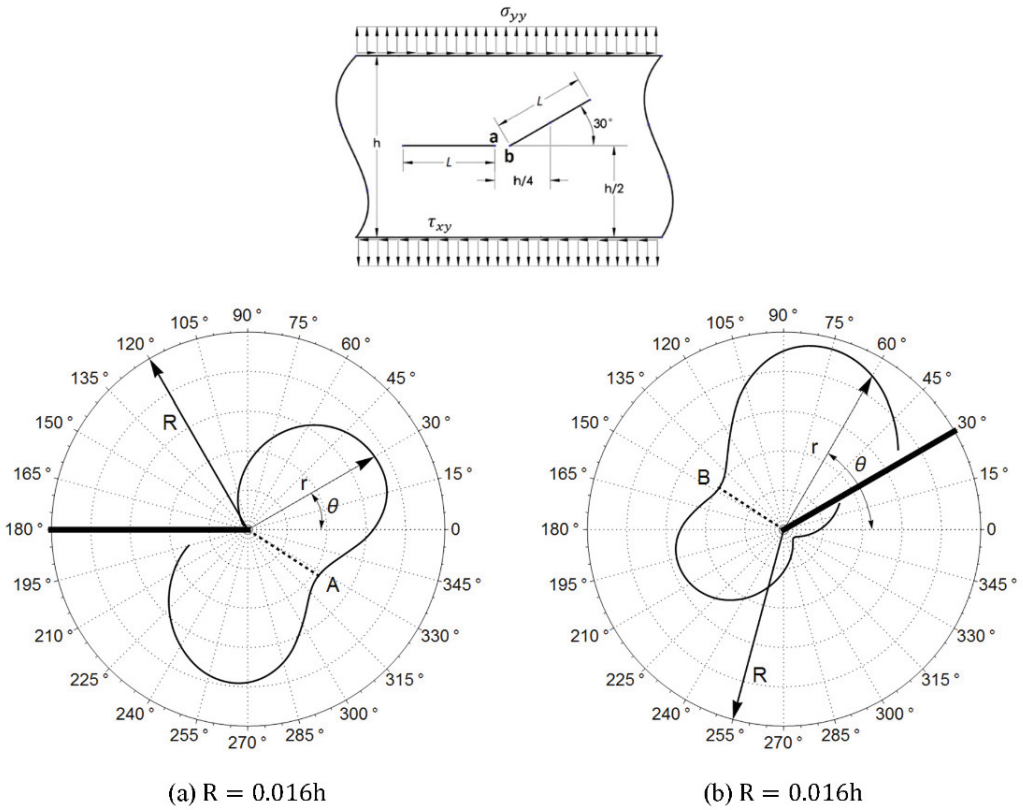

Fig. 6 Plastic zone and propagation angles of two interacting cracks

4. Conclusion

The distributed dislocation technique is used to derive integral equations for multiple cracks in a layer. These equations are solved numerically to determine the density of dislocation on a crack surface. Assuming small scale yielding, stress components are obtained in the vicinity of a crack tip. The stress components contain both singular and nonsingular terms. Utilizing von-Mises yield criterion and under plane-stress situation plastic region is specified around a crack tip. Comparing our results with those in the literature reveals that, in a cracked layer with a relatively large crack, the effects of nonsingular terms of stress field should not be neglected. Moreover, we observe that cracks propagate in the directions of the shortest lines connecting a crack tip to the boundary of plastic region experiencing tensile tangential stress.

Appendix A.

Functions in dislocation solution, Eq. (6), are

$$k_{xx}^{x}(x,y,\xi,\eta) = \lambda\frac{(y-\eta)[3(x-\xi)^2+(y-\eta)^2]}{[(x-\xi)^2+(y-\eta)^2]^2} + \lambda\int_0^\infty \left\{\frac{A_{11}}{\Delta}[2\cosh(\beta y)+\beta y\sinh(\beta y)] + \frac{A_{21}}{\Delta}[\beta y\cosh(\beta y)+\sinh(\beta y)] + [2-\beta(\eta-y)]e^{-\beta(\eta-y)}\right\}\cos[\beta(x-\xi)]\,d\beta$$

$$k_{xx}^{y}(x,y,\xi,\eta) = -\lambda\frac{(x-\xi)[(x-\xi)^2-(y-\eta)^2]}{[(x-\xi)^2+(y-\eta)^2]^2} + \lambda\int_0^\infty \left\{\frac{A_{12}}{\Delta}[2\cosh(\beta y)+\beta y\sinh(\beta y)] + \frac{A_{22}}{\Delta}[\beta y\cosh(\beta y)+\sinh(\beta y)] + [1-\beta(\eta-y)]e^{-\beta(\eta-y)}\right\}\sin[\beta(x-\xi)]\,d\beta$$

$$k_{yy}^{x}(x,y,\xi,\eta) = -\lambda\frac{(y-\eta)[(x-\xi)^2-(y-\eta)^2]}{[(x-\xi)^2+(y-\eta)^2]^2} - \lambda\int_0^\infty \left\{\frac{A_{11}}{\Delta}\beta y\sinh(\beta y) + \frac{A_{21}}{\Delta}[\beta y\cosh(\beta y)-\sinh(\beta y)] - \beta(\eta-y)e^{-\beta(\eta-y)}\right\}\cos[\beta(x-\xi)]\,d\beta$$

$$k_{yy}^{y}(x,y,\xi,\eta) = -\lambda\frac{(x-\xi)[(x-\xi)^2+3(y-\eta)^2]}{[(x-\xi)^2+(y-\eta)^2]^2} - \lambda\int_0^\infty \left\{\frac{A_{12}}{\Delta}\beta y\sinh(\beta y) + \frac{A_{22}}{\Delta}[\beta y\cosh(\beta y)-\sinh(\beta y)] - [1+\beta(\eta-y)]e^{-\beta(\eta-y)}\right\}\sin[\beta(x-\xi)]\,d\beta$$

$$k_{xy}^{x}(x,y,\xi,\eta) = -\lambda\frac{(x-\xi)[(x-\xi)^2-(y-\eta)^2]}{[(x-\xi)^2+(y-\eta)^2]^2} + \lambda\int_0^\infty \left\{\frac{A_{11}}{\Delta}[\beta y\cosh(\beta y)+\sinh(\beta y)] + \frac{A_{21}}{\Delta}\beta y\sinh(\beta y) + [1-\beta(\eta-y)]e^{-\beta(\eta-y)}\right\}\sin[\beta(x-\xi)]\,d\beta$$

$$k_{xy}^{y}(x,y,\xi,\eta) = -\lambda\frac{(y-\eta)[(x-\xi)^2-(y-\eta)^2]}{[(x-\xi)^2+(y-\eta)^2]^2} - \lambda\int_0^\infty \left\{\frac{A_{12}}{\Delta}[\beta y\cosh(\beta y)+\sinh(\beta y)] + \frac{A_{22}}{\Delta}\beta y\sinh(\beta y) - \beta(\eta-y)e^{-\beta(\eta-y)}\right\}\cos[\beta(x-\xi)]\,d\beta$$

$$0 < y < \eta$$

$$k_{xx}^{x}(x,y,\xi,\eta) = \lambda\frac{(y-\eta)[3(x-\xi)^2+(y-\eta)^2]}{[(x-\xi)^2+(y-\eta)^2]^2} + \lambda\int_0^\infty \left\{\frac{A_{31}}{\Delta}[2\cosh[\beta(h-y)]+\beta(h-y)\sinh[\beta(h-y)]] - \frac{A_{41}}{\Delta}[\beta(h-y)\cosh[\beta(h-y)]+\sinh[\beta(h-y)]] - [2+\beta(\eta-y)]e^{\beta(\eta-y)}\right\}\cos[\beta(x-\xi)]\,d\beta$$

$$k_{xx}^{y}(x,y,\xi,\eta) = -\lambda\frac{(x-\xi)[(x-\xi)^2-(y-\eta)^2]}{[(x-\xi)^2+(y-\eta)^2]^2} + \lambda\int_0^\infty \left\{\frac{A_{32}}{\Delta}[2\cosh[\beta(h-y)]+\beta(h-y)\sinh[\beta(h-y)]] - \frac{A_{42}}{\Delta}[\beta(h-y)\cosh[\beta(h-y)]+\sinh[\beta(h-y)]] + [1+\beta(\eta-y)]e^{\beta(\eta-y)}\right\}\sin[\beta(x-\xi)]\,d\beta$$

$$k_{yy}^{x}(x,y,\xi,\eta) = -\lambda\frac{(y-\eta)[(x-\xi)^2-(y-\eta)^2]}{[(x-\xi)^2+(y-\eta)^2]^2} - \lambda\int_0^\infty \left\{\frac{A_{31}}{\Delta}\beta(h-y)\,sinh[\beta(h-y)] - \frac{A_{41}}{\Delta}[\beta(h-y)\,cosh[\beta(h-y)] - sinh[\beta(h-y)]] - \beta(\eta-y)e^{\beta(\eta-y)}\right\} cos[\beta(x-\xi)]\,d\beta$$

$$k_{yy}^{y}(x,y,\xi,\eta) = -\lambda\frac{(x-\xi)[(x-\xi)^2+3(y-\eta)^2]}{[(x-\xi)^2+(y-\eta)^2]^2} - \lambda\int_0^\infty \left\{\frac{A_{32}}{\Delta}\beta(h-y)\,sinh[\beta(h-y)] - \frac{A_{42}}{\Delta}[\beta(h-y)\,cosh[\beta(h-y)] - sinh[\beta(h-y)]] - [1-\beta(\eta-y)]e^{\beta(\eta-y)}\right\} sin[\beta(x-\xi)]\,d\beta$$

$$k_{xy}^{x}(x,y,\xi,\eta) = -\lambda\frac{(x-\xi)[(x-\xi)^2-(y-\eta)^2]}{[(x-\xi)^2+(y-\eta)^2]^2} - \lambda\int_0^\infty \left\{\frac{A_{31}}{\Delta}[\beta(h-y)\,cosh[\beta(h-y)] + sinh[\beta(h-y)]] - \frac{A_{41}}{\Delta}\beta(h-y)\,sinh[\beta(h-y)] - [1+\beta(\eta-y)]e^{\beta(\eta-y)}\right\} sin[\beta(x-\xi)]\,d\beta$$

$$k_{xy}^{y}(x,y,\xi,\eta) = -\lambda\frac{(y-\eta)[(x-\xi)^2-(y-\eta)^2]}{[(x-\xi)^2+(y-\eta)^2]^2} + \lambda\int_0^\infty \left\{\frac{A_{32}}{\Delta}[\beta(h-y)\,cosh[\beta(h-y)] + sinh[\beta(h-y)]] - \frac{A_{42}}{\Delta}\beta(h-y)\,sinh[\beta(h-y)] + \beta(\eta-y)e^{\beta(\eta-y)}\right\} cos[\beta(x-\xi)]\,d\beta,$$

$$\eta < y < h$$

where

$$A_{11} = 8\{\beta h[\beta(h-\eta)\,cosh(\beta\eta) - sinh(\beta\eta)] - (sinh[\beta(h-\eta)] - \beta\eta\,cosh[\beta(h-\eta)])\,sinh(\beta h)\}$$

$$A_{12} = -8\beta\{\beta h(h-\eta)\,sinh(\beta h) - \eta\,sinh[\beta(h-\eta)]\,sinh(\beta h)\}$$

$$A_{21} = -8\beta\{\beta h(h-\eta)\,sinh(\beta h) + \eta\,sinh[\beta(h-\eta)]\,sinh(\beta h)\}$$

$$A_{22} = 8\{\beta h[\beta(h-\eta)\,cosh(\beta\eta) + sinh(\beta\eta)] - (sinh[\beta(h-\eta)] + \beta\eta\,cosh[\beta(h-\eta)])\,sinh(\beta h)\}$$

$$A_{31} = -8\{\beta h[\beta\eta\,cosh[\beta(h-\eta)] + sinh(\beta\eta)\,cosh(\beta h)] - [sinh(\beta\eta) + \beta\eta\,cosh(\beta\eta)]\,sinh(\beta h)\}$$

$$A_{32} = -8\beta\{\beta h\eta\,sinh[\beta(h-\eta)] - (h-\eta)\,sinh(\beta\eta)\,sinh(\beta h)\}$$

$$A_{41} = -8\beta\{\beta h\eta\,sinh[\beta(h-\eta)] + (h-\eta)\,sinh(\beta\eta)\,sinh(\beta h)\}$$

$$A_{42} = -8\{\beta h[\beta\eta\,cosh[\beta(h-\eta)] - sinh(\beta\eta)\,cosh(\beta h)] - [sinh(\beta\eta) - \beta\eta\,cosh(\beta\eta)]\,sinh(\beta h)\}$$

$$\Delta = sinh^2(\beta h) - \beta^2 h^2, \qquad \lambda = \frac{\mu}{2\pi(\kappa+1)}$$

References

Banks, T. M., Garlick, A., 1984. The form of crack tip plastic zones, Engineering Fracture Mechanics 19(3), 571-581.

Bian, L. -C., Kim, K. S., 2004. The minimum plastic zone radius criterion for crack initiation direction applied to surface cracks and through-cracks under mixed mode loading, International Journal of Fatigue 26(11), 1169-1178.

Dugdale, D. S., 1960. Yielding of steel sheets containing slits, Journal of the Mechanics and Physics of Solids 8(2), 100-104.

Erdogan, F., Sih, G. C., 1963. On the Crack Extension in Plates Under Plane Loading and Transverse Shear, Journal of Basic Engineering 85(4), 519-525.

Erdogan, F., Gupta, G. D., Cook, T. S., Numerical solution of integral equations, In: Sih G.C. (Ed.), 1973. Methods of Analysis and Solution of Crack Problems, Noordhoof, Leyden (Holland), 368-425.

Golos, K., Wasiluk, B., 2000. Role of plastic zone in crack growth direction criterion under mixed mode loading, International Journal of Fracture 102(4), 341-353.

Harmain, G. A., Provan, J. W., 1997. Fatigue crack-tip plasticity revisited - The issue of shape addressed, Theoretical and Applied Fracture Mechanics 26(2), 63-79.

Khan, S. M. A., Khraisheh, M. K., 2000. Analysis of mixed mode crack initiation angles under various loading conditions, Engineering Fracture Mechanics 67(5), 397-419.

Larsson, S. G., Carlsson, A. J., 1973. Influence of non-singular stress terms and specimen geometry on small-scale yielding at crack tips in elastic-plastic materials, Journal of the Mechanics and Physics of Solids 21(4), 263-277.

Neimitz, A., 2004. Modification of Dugdale model to include the work hardening and in- and out-of-plane constraints, Engineering Fracture Mechanics 71(11), 1585-1600.

Panasyuk, V., Savruk, M., 1992. Plastic strip model in elastic-plastic problems of fracture mechanics, Adv. Mech. 15(3), 123-147.

Zhu, P., Yang, L., Li, Z, Sun, J., 2010. The shielding effects of the crack-tip plastic zone, International Journal of Fracture 161(2), 131-139.